



Collisionless Diffusion of Particles and Current Across a Magnetic Field in Beam/Plasma Interaction

G. Manfredi, M. Shoucri, I. Shkarofsky, A. Ghizzo, P. Bertrand, E. Fijalkow, M. Feix, S. Karttunen, T. Pattikangas & R. Salomaa

To cite this article: G. Manfredi, M. Shoucri, I. Shkarofsky, A. Ghizzo, P. Bertrand, E. Fijalkow, M. Feix, S. Karttunen, T. Pattikangas & R. Salomaa (1996) Collisionless Diffusion of Particles and Current Across a Magnetic Field in Beam/Plasma Interaction, *Fusion Technology*, 29:2, 244-260, DOI: [10.13182/FST96-A30711](https://doi.org/10.13182/FST96-A30711)

To link to this article: <https://doi.org/10.13182/FST96-A30711>



Published online: 09 May 2017.



Submit your article to this journal [↗](#)



View related articles [↗](#)

COLLISIONLESS DIFFUSION OF PARTICLES AND CURRENT ACROSS A MAGNETIC FIELD IN BEAM/PLASMA INTERACTION

PLASMA HEATING
SYSTEMS

KEYWORDS: beam/plasma interaction, direct current helicity injection, collisionless diffusion

G. MANFREDI* and M. SHOUCRI *Centre canadien de fusion magnétique
Varennnes, Québec, Canada J3X1S1*

I. SHKAROFISKY *MPB Technologies Inc., Dorval, Québec, Canada H9P 1J1*

A. GHIZZO and P. BERTRAND *Université de Nancy
Laboratoire de Physique des Milieux Ionisés-URA835, Nancy, France*

E. FIJALKOW and M. FEIX *Université d'Orléans
Centre Nationale de la Recherche Scientifique, MAPMO-URA D 1803, France*

S. KARTTUNEN, T. PATTIKANGAS, and R. SALOMAA
Association Euratom-TEKES, VTT Energy, P.O. Box 1604, FIN-02044 VTT, Finland

Received January 20, 1995

Accepted for Publication August 18, 1995

A drift-kinetic Eulerian Vlasov code with fluid equations for the ions is used to study the collisionless diffusion of particles and current across a magnetic field for the case of an electron beam injected near the edge of a two-dimensional magnetized plasma slab. The case of a magnetic field tilted with respect to the beam direction at an angle of $\theta = 10$ deg is considered. Test particles diagnostic techniques are used to study the evolution of the phase space at different locations across the plasma slab. We analyze the anomalous diffusion process triggered by the beam-plasma instability and induced in space across the magnetic field by the Kelvin-Helmholtz instability and the velocity space diffusion induced along the magnetic field due

to the kinetic effects of the beam-plasma instability. In the present slab geometry it is found that the collisionless diffusion coefficients D_y and $D_{v_{\parallel}}$, describing respectively the anomalous diffusion in physical space and in velocity space, are related by the relation $D_y = D_{v_{\parallel}} \tan^2 \theta / \omega_{ce}^2$. This relation, which links the electron dynamics in the x - y real space and in the y - v_{\parallel} phase space, is verified accurately using the test particles diagnostic techniques. The Vlasov code associated with test particles techniques provides a powerful tool to study particle diffusion in space and in phase space, especially in the low-density regions of the distribution function.

I. INTRODUCTION

The injection of an electron beam into a confined plasma has proved to be an efficient method for plasma heating. This problem is also of importance in current drive experiments where an electron beam is injected into a plasma, also known as direct current (dc) helicity injection.¹ In these experiments, it is found that when the beam density is a few percent of the back-

ground plasma density, a significant amount of beam and background electrons is accelerated considerably beyond the initial beam velocity and diffuse in space across the magnetic field. Beam/plasma interactions have long been studied to investigate plasma diffusion in velocity space.²⁻⁴ However, the diffusion in space of electrons in the presence of a beam-plasma instability has received little attention. With this in mind, we mention the recent experimental results reported in Ref. 5.

A study of the problems related to anomalous diffusion across a magnetic field caused by the injection

*Current address: Culham Laboratory, Abingdon, England.

of an electron beam necessitates a good understanding of the basic physical processes involved in the competition and cross effects between the kinetic beam-plasma instability and the Kelvin-Helmholtz instability generated simultaneously by the shear in the $\mathbf{E} \times \mathbf{B}$ drift. Several numerical simulations have tried to address these problems and to investigate the details of the anomalous transport induced by $\mathbf{E} \times \mathbf{B}$ instabilities when a beam is injected in a plasma.⁶⁻⁸ Instabilities associated with $\mathbf{E} \times \mathbf{B}$ drift are conjectured to be one of the important mechanisms for anomalous transport in the plasma. However, in many of the simulations employing particle-in-cell (PIC) techniques, the PIC codes lack an adequate number of simulation particles to display the detailed phase-space structure of the distribution function, especially in those regions of phase space where trapping occurs. Recently, a drift-kinetic Vlasov equation was developed⁹ and applied to study the Kelvin-Helmholtz instability and the η_i instability that can give rise to convective cells at the edge of plasma. Furthermore, this code was applied to study the diffusion across a magnetic field in a beam/plasma interaction,¹⁰ for different angle θ between the magnetic field and the x axis. A powerful technique that consists of following the trajectories of test particles (we have chosen here 4096 particles) using the electric field computed by the Vlasov code, has been developed to study the diffusion of particles in space and velocity space. In the results in Ref. 10, particular attention was given to particles located in velocity space in the beam region

to study how beam particles accelerate and diffuse under the mechanism of beam-plasma instability. It gave a powerful phase-space representation of the effect of the instability on the beam. In the present work, we restrict ourselves to the case $\theta = 10$ deg, which is more relevant to the problem of dc helicity injection. We will consider the heating and diffusion of particles not only in the beam region but also close to the bulk of the Maxwellian distribution and at different locations in the slab. This will provide an interesting picture on the heating, acceleration, and diffusion of the particles initially located in different position in phase space during the mechanism triggered by the beam-plasma instability. These results are not restricted to the case where the beam-plasma instability is the triggering mechanism for the acceleration of particles: They also apply in any situation where particles are accelerated in velocity space, e.g., in lower hybrid current drive for instance. Indeed, work is in progress to apply a similar drift-kinetic Vlasov code with a similar slab model to the problem of lower hybrid current drive.¹¹

II. THE MODEL AND PERTINENT EQUATIONS

The model and pertinent equations have been previously reported.^{9,10} The pertinent equations are written in order to fix the notation. The electron kinetic effects are included in the model in order to take into account the physics associated with the electrons generated by the beam-plasma instability. Fluid equations are used for the ions. The slab geometry used is shown in Fig. 1. The plasma is assumed periodic in the x direction with periodicity L_x and finite in the y direction. The magnetic field $\mathbf{B} = (B_x, \theta, B_z)$ makes an angle θ with the x direction. The electron distribution function $f_e(x, y, v_{\parallel}, t)$ obeys the drift-kinetic Vlasov equation that, for the system of coordinates considered, is written:

$$\frac{\partial f_e}{\partial t} + \left(v_{\parallel} \cos \theta + E_y \frac{\sin \theta}{\omega_{ce}} \right) \frac{\partial f_e}{\partial x} - \frac{E_x \sin \theta}{\omega_{ce}} \frac{\partial f_e}{\partial y} - E_x \cos \theta \frac{\partial f_e}{\partial v_{\parallel}} = 0. \quad (1)$$

In this equation, v_{\parallel} denotes the velocity of electrons along the magnetic field, normalized to the thermal velocity $v_{Te} = (T_e/m_e)^{1/2}$. The distances are normalized to the electron Debye length λ_{De} , and the time t is normalized to the inverse plasma frequency ω_{pe}^{-1} ; ω_{ce} is the electron cyclotron frequency, in units of ω_{pe} .

The ion motion is described using a guiding center approximation for the ion density that in our normalized units is written:

$$\frac{\partial n_i}{\partial t} + E_y \frac{\sin \theta}{\omega_{ce}} \frac{\partial n_i}{\partial x} - E_x \frac{\sin \theta}{\omega_{ce}} \frac{\partial n_i}{\partial y} = 0. \quad (2)$$

We have neglected the motion of the heavy ions along the magnetic field.

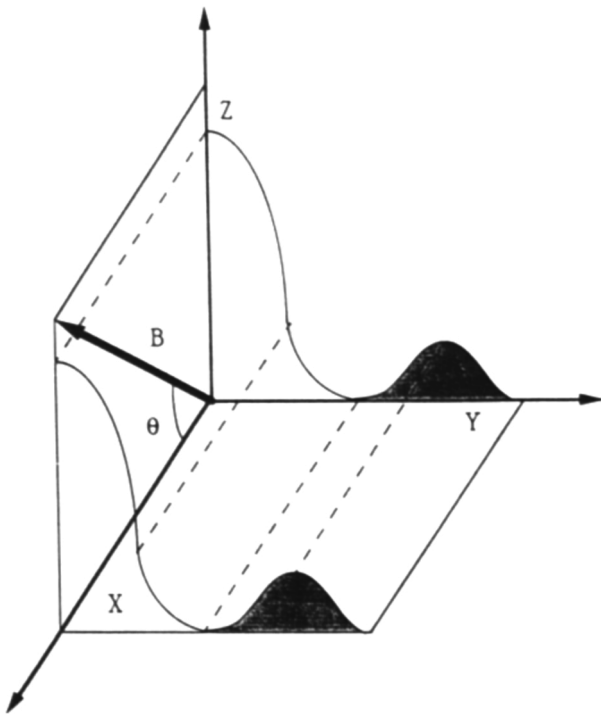


Fig. 1. Slab geometry used for the simulation.

In the present simulation, we take $\theta = 10$ deg. We have a grid for v_{\parallel} such that $-6v_{te} < v_{\parallel} < 12v_{te}$ and the space coordinates are chosen such that $0 < x < L_x$ and $-L_y < y < L_y$. The field components E_x and E_y are obtained from the electric potential using Poisson's equation:

$$\Delta\phi = n_i(x, y, t) - n_e(x, y, t) \quad (3)$$

and

$$E_x = -\frac{\partial\phi}{\partial x}, \quad E_y = -\frac{\partial\phi}{\partial y},$$

where

$$n_e(x, y, t) = \int_{-\infty}^{\infty} f_e(x, y, v_{\parallel}, t) dv_{\parallel}. \quad (4)$$

The solution of these equations uses a method of fractional steps associated with cubic spline interpolation.

The main steps for the numerical solution of these equations have been reported in Refs. 9 and 10. The simulation presented here has been performed with a phase-space grid of $N_x N_y N_{v_{\parallel}} = 128 \times 128 \times 256$, i.e., the equivalent of 4 194 304 "particles" for the description of the electron distribution function on phase space. The time step used is $\Delta t \omega_{pe} = 0.05$, and the CPU time necessary to compute the plasma evolution until $t \omega_{pe} = 60$ is ~ 5 h on a CRAY-2 computer, which is equivalent to $3.5 \mu\text{s}$ per time step per particle.

The initial condition for the electron distribution function is given by

$$f_e(x, y, v_{\parallel}, t) = \left[\frac{n_o(y)}{\sqrt{2\pi}} e^{-v_{\parallel}^2/2} + \frac{n_b(y)}{\sqrt{2\pi v_{tb}}} e^{-(v_{\parallel} - v_b)^2} \right] \times (1 + \epsilon \sin k_o x). \quad (5)$$

The initial condition for the ion density is given by

$$n_i(x, y, t = 0) = n_o(y) (1 + \epsilon \sin k_o x), \quad (6)$$

where $k_o = 2\pi/L_x$ denotes the fundamental wavenumber and $n_o(y)$ denotes the background density profile:

$$n_o(y) = \frac{\sqrt{\beta}}{\sqrt{2\pi}} e^{-\beta y^2} \quad (7)$$

with $\beta = 0.025$.

The beam density is

$$n_b(y) = C \operatorname{sech}[(y - y_b)/a] \quad (8)$$

with $a = 0.9$ and $y_b = -6$ in Debye length units.

The integral

$$\frac{1}{2L_y} \int_{-L_y}^{L_y} n_b(y) dy = 0.14 \quad (9)$$

determines C . We also use $L_x = 40$ and $2L_y = 30$. We take $\omega_{ce} = \omega_{pe}$, and for the initial perturbation amplitude in Eqs. (5) and (6) we take $\epsilon = 0.2$. The electron beam velocity along the magnetic field is $v_b = 6.75 v_{Te}$ with a thermal velocity $v_{tb} = 0.7 v_{Te}$. The electrostatic potential is set equal to zero at the finite boundary $y = \pm L_y$.

III. RESULTS

We study the evolution of the beam-plasma instability and concentrate in this section on the trajectories of 4096 test particles initially located around the beam region. The trajectories of the electrons in phase space are obtained by integrating the equations of motion along the characteristics of the Vlasov Eq. (1);

$$\frac{dx}{dt} = v_{\parallel} \cos \theta + E_y \frac{\sin \theta}{\omega_{ce}}, \quad (10)$$

$$\frac{dy}{dt} = -E_x \frac{\sin \theta}{\omega_{ce}}, \quad (11)$$

and

$$\frac{dv_{\parallel}}{dt} = -E_x \cos \theta. \quad (12)$$

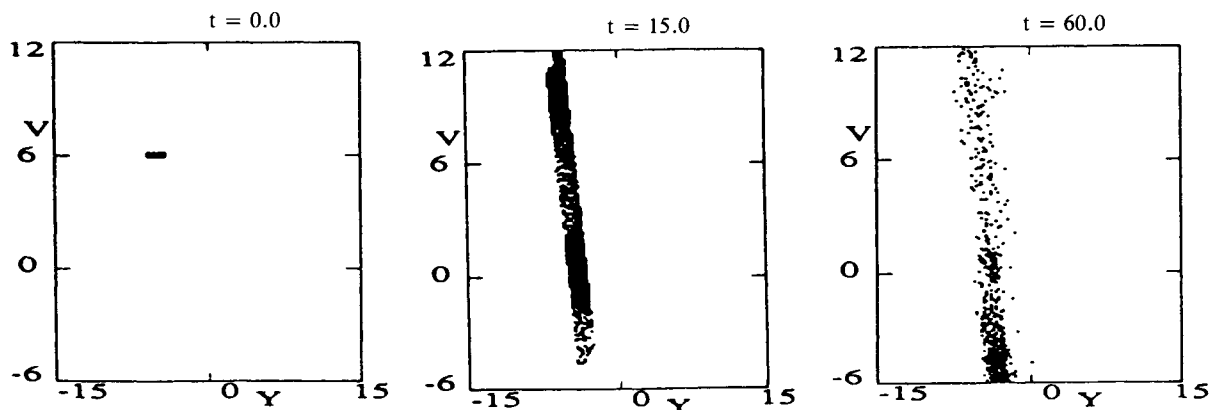


Fig. 2. Time evolution of $N = 4096$ test particles initially located in the beam around $y_b = -6\lambda_{De}$, $v_b = +6.75 v_{Te}$, in the y - v_{\parallel} phase space.

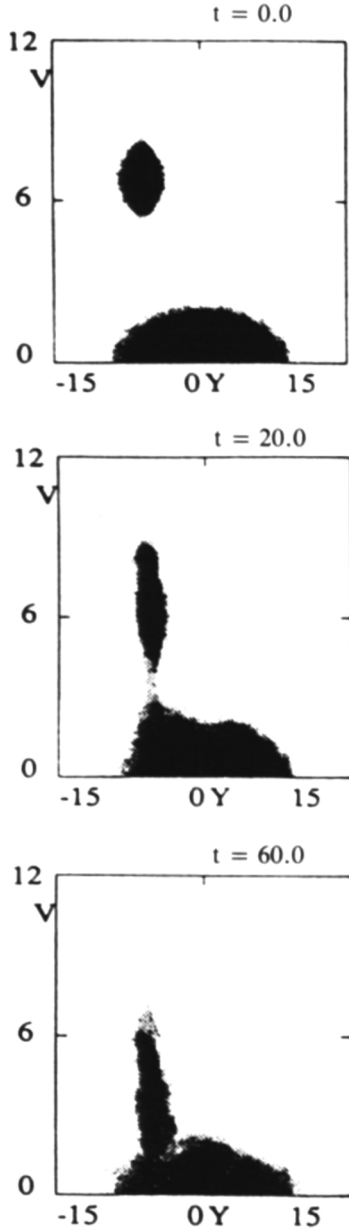


Fig. 3. Shadow plot of the time evolution of the distribution function in the y - $v_{||}$ phase space.

Equations (11) and (12) can readily be integrated to give

$$y - y_o = \frac{\tan \theta}{\omega_{ce}} (v_{||} - v_{||o}), \quad (13)$$

where $v_{||o}$ and y_o are the coordinates of the initial position. Equation (13) follows also from the conservation of the z component of the canonical momentum $P_z = mv_z + eA_z$, with $A_z = -B_x y$ and $v_z = v_{||} \sin \theta$. Equation (13) has been numerically verified by following the trajectories of the distribution of test particles taken initially at different positions in the slab, in the

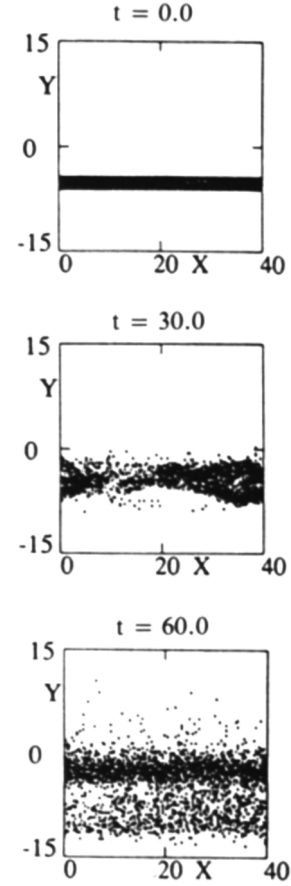


Fig. 4. Time evolution of $N = 4096$ test particles initially located in the beam around $y_b = -6\lambda_{De}$, in the x - y plane.

self-consistent field calculated by the Vlasov-Poisson system of equations. This technique has been described in recent publications.^{10,12} Equations (10), (11), and (12) are integrated for the N test electrons using the following leapfrog scheme:

$$x^{n+1/2} = x^{n-1/2} + \Delta t \left(v_{||}^n + E_y^n \frac{\sin \theta}{\omega_{ce}} \right), \quad (14a)$$

$$y^{n+1/2} = y^{n-1/2} - \Delta t E_x^n \frac{\sin \theta}{\omega_{ce}}, \quad (14b)$$

and

$$v_{||}^{n+1} = v_{||}^n - E_x^{n+1/2} \cos \theta \Delta t. \quad (14c)$$

The positions of each particle at time t_{n+1} are calculated using the relations:

$$\begin{aligned} x^{n+1} &= x^{n+1/2} + \frac{1}{2} \Delta t \left(\frac{\partial x}{\partial t} \right)^{n+1/2} \\ &\approx x^{n+1/2} + \frac{1}{2} \Delta t \left(v_{||}^n \cos \theta + E_y^n \frac{\sin \theta}{\omega_{ce}} \right), \end{aligned} \quad (15a)$$

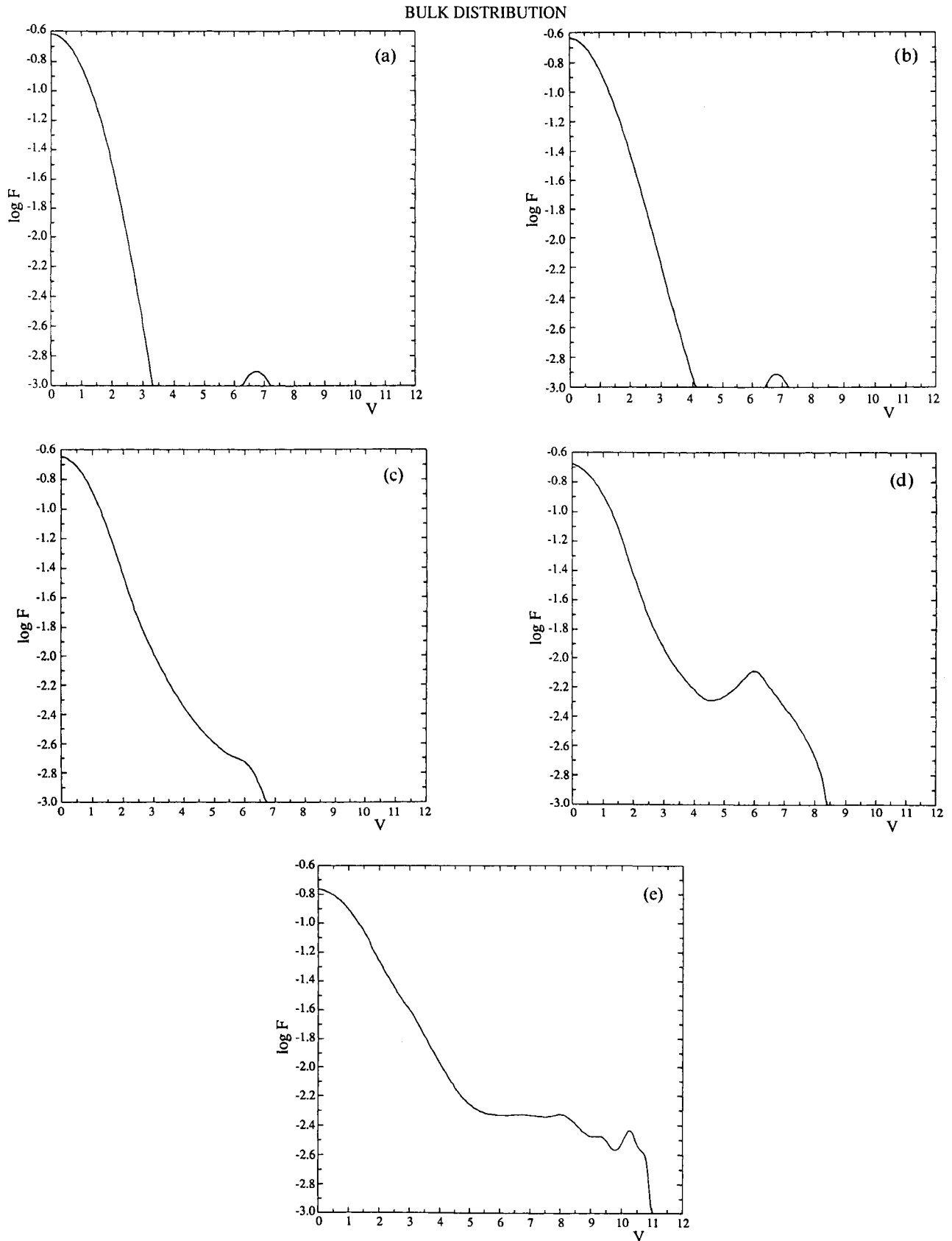


Fig. 5. Spatially averaged distribution function around the center as defined in Eq. (21) at (a) $t = 0$, (b) $t = 15$, (c) $t = 20$, (d) $t = 35$, and (e) $t = 60$.

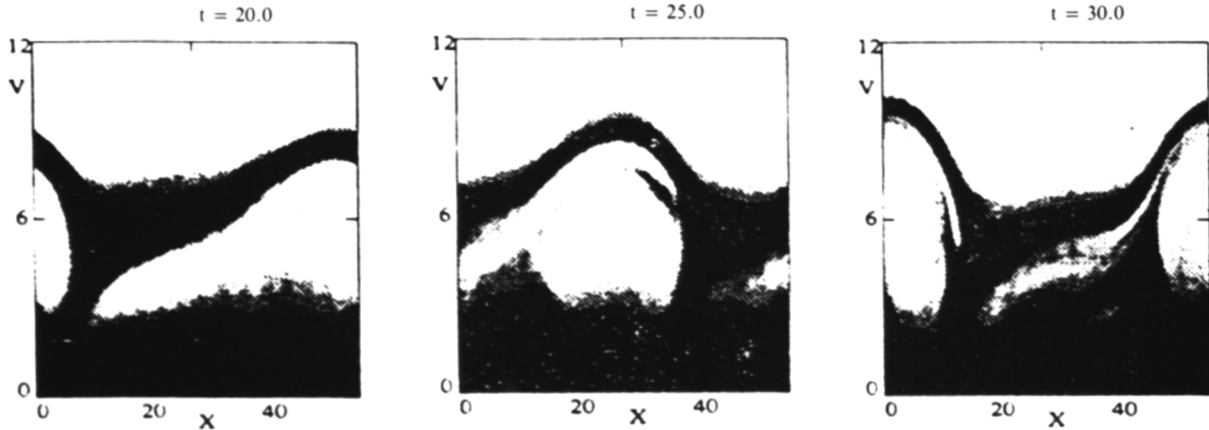


Fig. 6. Shadow plot of the time evolution of the distribution function in the x - $v_{||}$ phase space.

and

$$y^{n+1} = y^{n+1/2} + \frac{1}{2} \Delta t \left(\frac{\partial y}{\partial t} \right)^{n+1/2} \approx y^{n+1/2} + \frac{1}{2} \Delta t \left(-E_x^n \frac{\sin \theta}{\omega_{ce}} \right). \quad (15b)$$

In the aforementioned relations, the field E_x^n , E_y^n , and $E_x^{n+1/2}$ components are known at t_n and $t_{n+1/2}$ since they have already been computed at grid points in the numerical simulation using the Vlasov code and subsequently stored.

The result of the phase space $v_{||}$ - y is shown in Fig. 2 for the $N = 4096$ test particles taken initially among the beam electrons injected around $y_b \sim -6$ and $v_b \sim 6$. The initial location of these test particles is shown in Fig. 2 at $t = 0$. The evolution in time confirms the straight line motion given by Eq. (13). Note how electrons are moving rapidly along both directions of the

initial position. At $t = 15$, some electrons have already reached and crossed the Maxwellian bulk centered at $v_{||} = 0$. At $v_{||} \sim -6v_{Te}$, we expect from Eq. (13) $y \sim -4$, in good agreement with the results in Fig. 2. These results are also confirmed by the shadow plot of the time evolution of the distribution function during the simulation, in the y - $v_{||}$ phase space presented in Fig. 3, which also shows particles being accelerated from the plasma bulk. Since we have no collisions in the present simulation, note how by conserving the canonical momentum P_z , energetic electrons can reach the Maxwellian bulk without being thermalized, while at the same time the Maxwellian bulk is heated and particles are being accelerated.

The diffusion coefficients D_y and $D_{v_{||}}$ have been calculated, where D_y denotes the diffusion across the magnetic field (along the y direction) and $D_{v_{||}}$ denotes the diffusion in the $v_{||}$ direction. We compute D_y from the measurement of the quantity $\langle (\Delta y)^2 \rangle$ for the set of $N = 4096$ test particles:

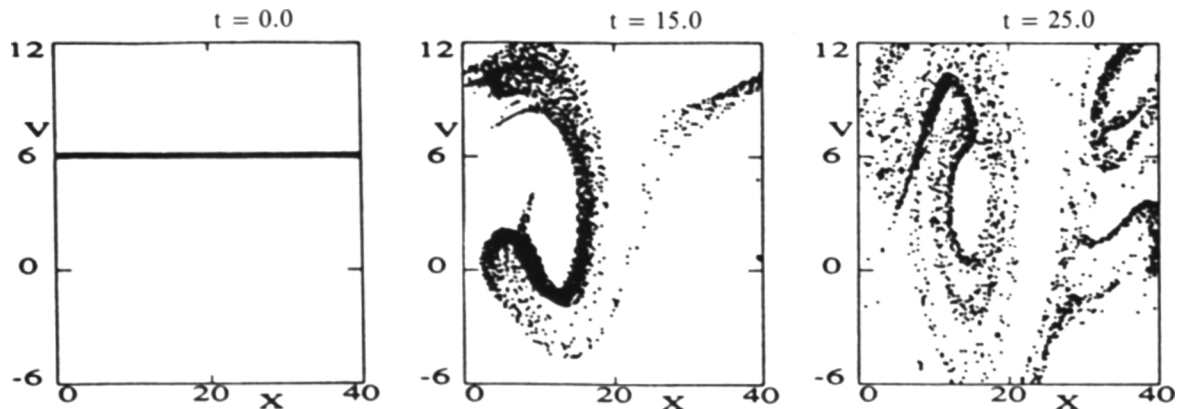


Fig. 7. Time evolution of $N = 4096$ test particles initially located in the beam around $v_b = 6.75v_{Te}$, in the x - $v_{||}$ phase space.

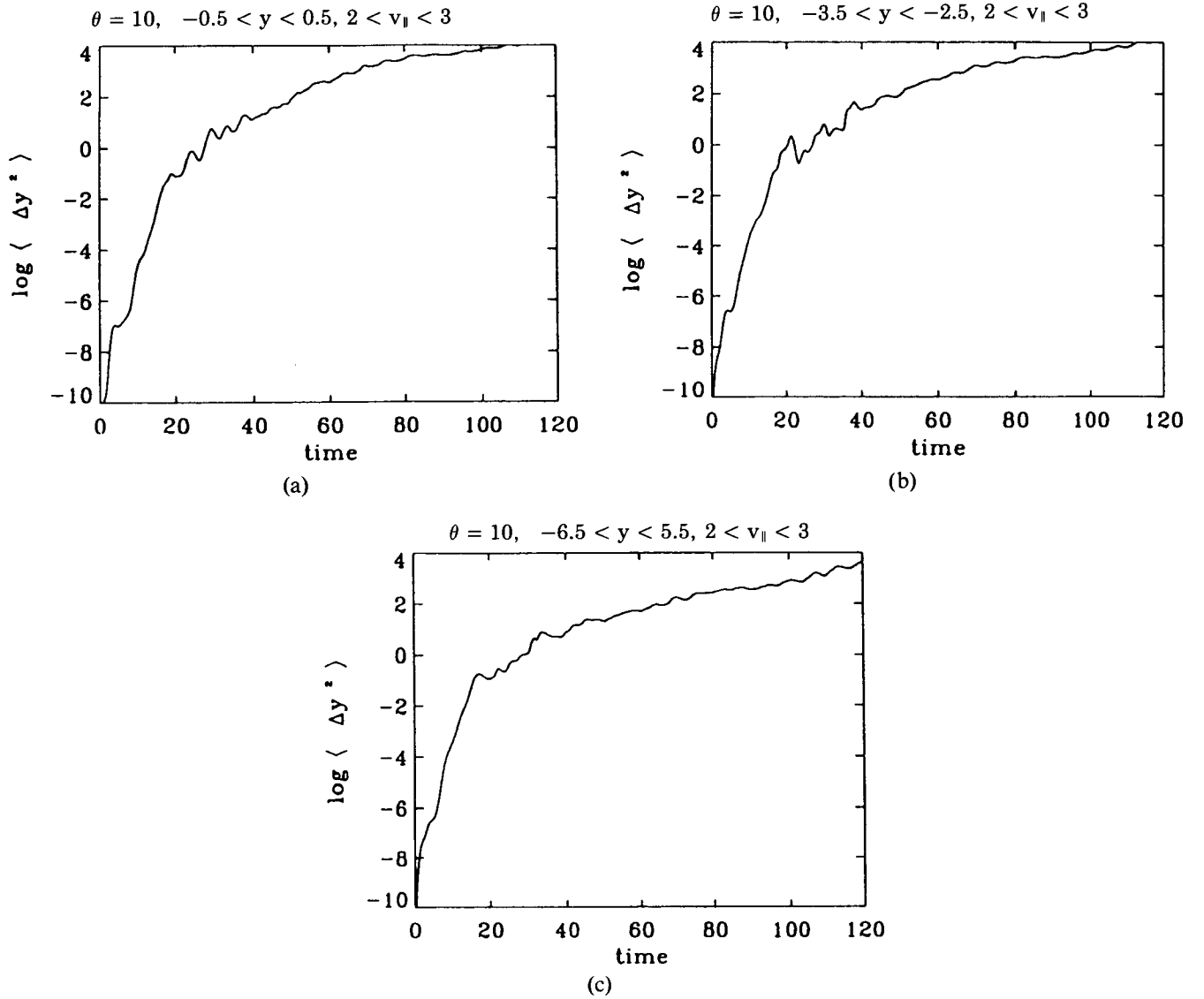


Fig. 8. Plot of $\langle (\Delta y)^2 \rangle$ as defined in Eq. (16) on a logarithmic scale for the test particles located in velocity space at $2 < v_{\parallel} < 3$ and in space at (a) $-0.5 < y < 0.5$, (b) $-3.5 < y < -2.5$, and (c) $-6.5 < y < -5.5$.

$$\langle (\Delta y)^2 \rangle = \frac{1}{N} \sum_{i=1}^N [y_i(t) - y_i(o)]^2 \quad (16)$$

which denotes the average square displacement of the electrons from their initial positions. Then, D_y is defined by the quantity:

$$D_y = \frac{1}{2t} \langle (\Delta y)^2 \rangle. \quad (17)$$

In a similar way, we define

$$\langle (\Delta v_{\parallel})^2 \rangle = \frac{1}{N} \sum_{i=1}^N [v_{\parallel i}(t) - v_{\parallel i}(o)]^2 \quad (18)$$

and

$$D_{v_{\parallel}} = \frac{1}{2t} \langle (\Delta v_{\parallel})^2 \rangle. \quad (19)$$

From Eqs. (16) through (19) and Eq. (13), we derive the following relation:

$$D_y = D_{v_{\parallel}} \tan^2 \theta / \omega_{ce}^2. \quad (20)$$

Equation (20), relating the diffusion in space across the magnetic field to the diffusion in velocity space for the collisionless plasma model we are studying, has been accurately verified for the 4096 test particles as will be seen in Sec. IV. More interesting is the behavior of

the 4096 test particles in the x - y plane. Figure 4 shows at $t = 0$ the beam initially located around $y_b = -6$ as indicated by Eq. (8). Figure 4 shows the beam diffusing almost coherently toward the center of the plasma, up the gradient of the plasma density. This diffusion of the particles is also accompanied by a diffusion of the current toward the plasma center, and by the distribution function at the center heating, and particles getting accelerated. This is confirmed by the study of the spatially averaged distribution around the plasma center. Figure 5 shows the time evolution of the spatially averaged distribution function:

$$F(v_{\parallel}) = \int_{-2.5}^{2.5} dy \int_0^{L_x} dx f(x, y, v_{\parallel}) / L_x \quad (21)$$

in a strip of width $5\lambda_{De}$ around the center $y = 0$. A very small bump in the tail, as given by Eq. (8), is seen in Fig. 5a at $t = 0$, since the beam is essentially located initially around $y_b = -6$. In spite of the very rapid evolution of the bump-in-tail instability for the beam located around $y_b = -6$ as indicated by Figs. 2, 3, and 4, the result in Fig. 5b at $t = 15$ shows the spatially averaged beam population in the region around the center of the plasma evolving only slightly. However, a

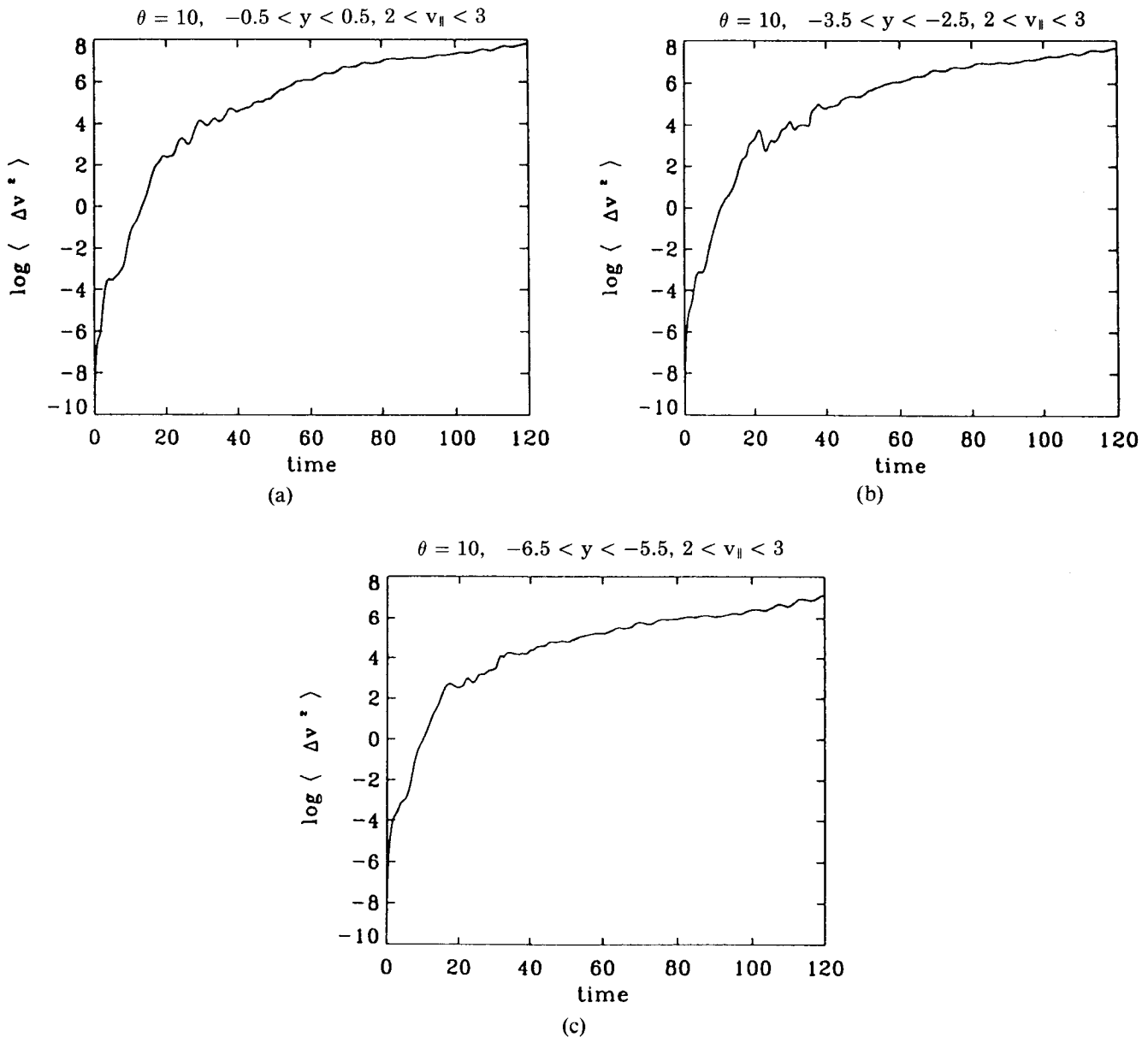


Fig. 9. Plot of $\langle (\Delta v_{\parallel})^2 \rangle$ as defined in Eq. (18) on a logarithmic scale for the test particles located in velocity space at (a) $-0.5 < y < 0.5$, (b) $-3.5 < y < -2.5$, and (c) $-6.5 < y < -5.5$.

noticeable heating of the plasma bulk is already apparent in Fig. 5b. The coupling with the $\mathbf{E} \times \mathbf{B}$ drift and the diffusion from neighboring layers are important. This initial phase is followed by a phase in which the cross effect of the growing beam-plasma instability with $\mathbf{E} \times \mathbf{B}$ motion heats and accelerates particles as apparent in Figs. 5c, 5d, and 5e. A shadow plot of the x - v_{\parallel} phase space in Fig. 6 shows the rapid formation of a big vortex structure, extending over all the tail of

the distribution function corresponding to the accelerated particles shown in Fig. 5e. From Fig. 6 at $t = 20, 25$, and 30 , the peak of the vortex is moving a distance of ~ 25 in a period $t = 5$, corresponding to a phase velocity $v_{ph} \sim 25/5 \sim 5$. Since the wavenumber is $k_x = 2\pi/40$, this corresponds to a frequency $\omega/\omega_{pe} \sim 5 \times 2\pi/40 \sim 0.8$ for the most unstable mode. The center of the vortex is located around $v_{\parallel} \approx 5$, in agreement with the value of the phase velocity. Figure 7 shows the same

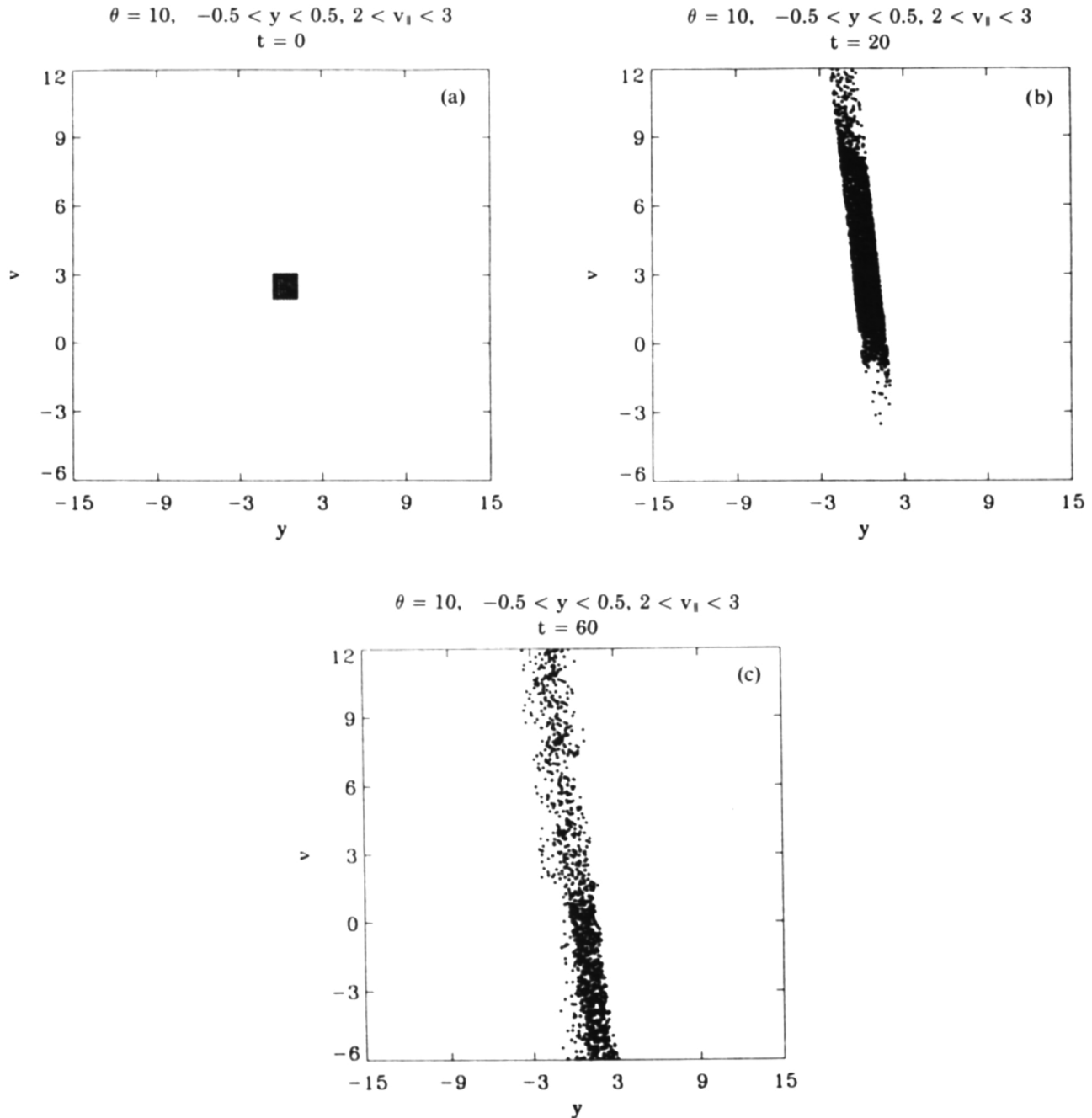


Fig. 10. Evolution of the v_{\parallel} - y phase space for the 4096 test particles initially located at $-0.5 < y < 0.5$ at (a) $t = 0$, (b) $t = 20$, and (c) $t = 60$.

x - v_{\parallel} phase space, for the $N = 4096$ test particles originally located at $t = 0$ in the beam region, around $v_b \sim 6$. The particles are following the rapid formation and evolution of a big vortex throughout the v_{\parallel} - x space. We conclude this section by pointing again to the huge tail in Fig. 5e formed in the spatially averaged distribution function around the center of the slab, while the beam was injected around $y = -6$.

IV. DIFFUSION OF PARTICLES CLOSE TO THE BULK OF THE MAXWELLIAN

In this section, the heating and acceleration of the particles close to the bulk of the Maxwellian distribution are examined. Three sets of 4096 particles were chosen close to the bulk of the plasma at $2 < v_{\parallel} < 3$, at three different locations in the slab: $-0.5 < y < 0.5$,

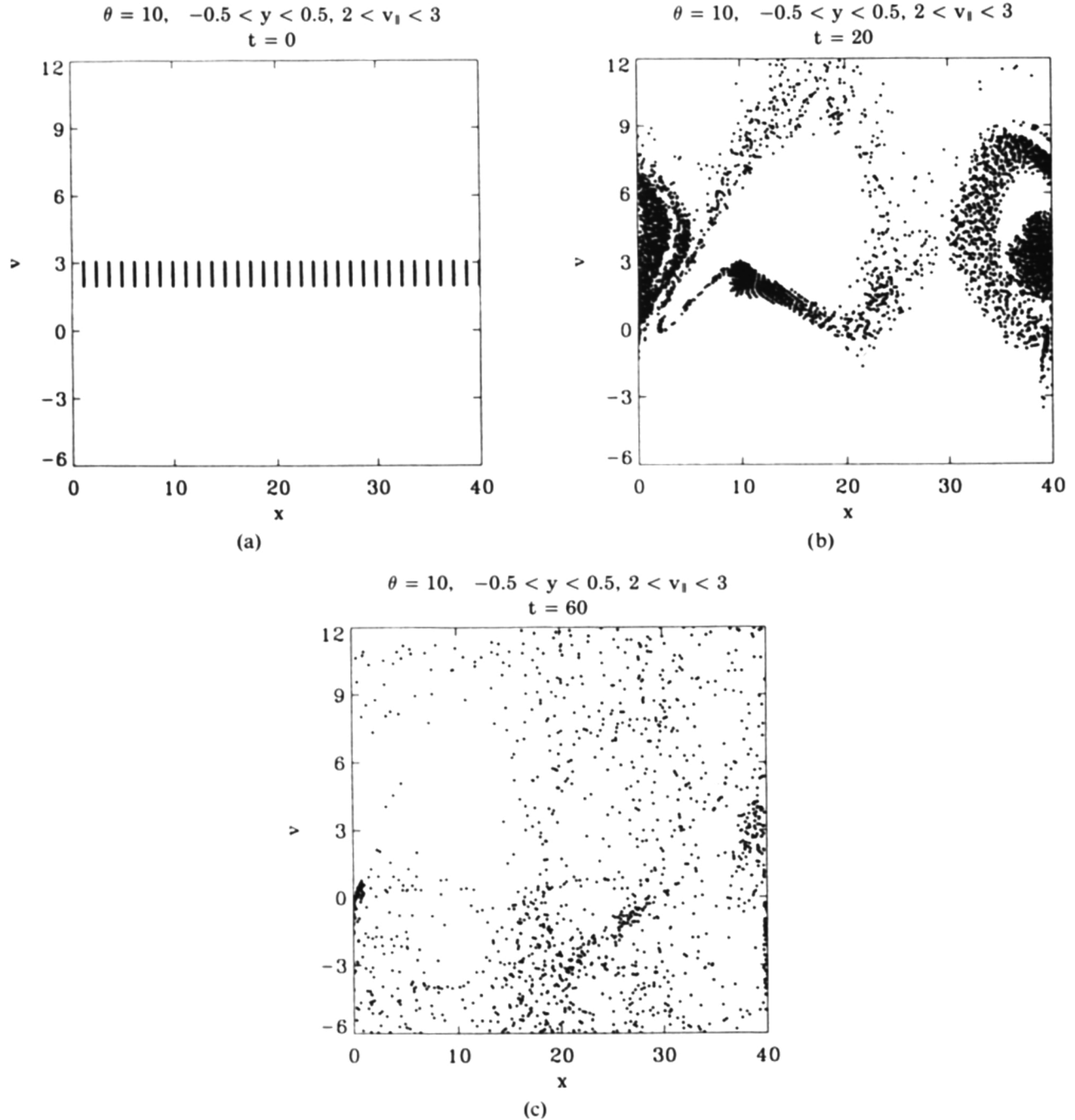


Fig. 11. Evolution of the v_{\parallel} - x phase space for the 4096 test particles initially located at $-0.5 < y < 0.5$ at (a) $t = 0$, (b) $t = 20$, and (c) $t = 60$.

$-3.5 < y < -2.5$, and $-6.5 < y < -5.5$. The values of $\langle(\Delta y)^2\rangle$ and $\langle(\Delta v_{\parallel})^2\rangle$ for the particles at these three locations, calculated from Eqs. (16) and (18), are plotted in Figs. 8 and 9 on a logarithmic scale. There is a clear tendency for an exponential behavior after $t = 40$ especially for the curves in Figs. 8c and 9c for the particles initially located in the beam region ($-6.5 < y < -5.5$), in which the exponential behavior seems to persist for a long time. (However, by this time, an important fraction of the particles have reached the boundary

in velocity space.) The curves in Figs. 8 and 9 show that the relation given in Eq. (20) is exactly verified. The evolution of these test particles in the v_{\parallel} - y space follows again very nicely the invariant calculated in Eq. (13), as shown in Fig. 10 for the particles located around the center ($-0.5 < y < 0.5$). The other particles show a similar behavior in the v_{\parallel} - y space. As early as $t = 20$, particles initially located close to the Maxwellian bulk at $2 < v_{\parallel} < 3$ experience strong acceleration toward the tail of the distribution function as well as strong

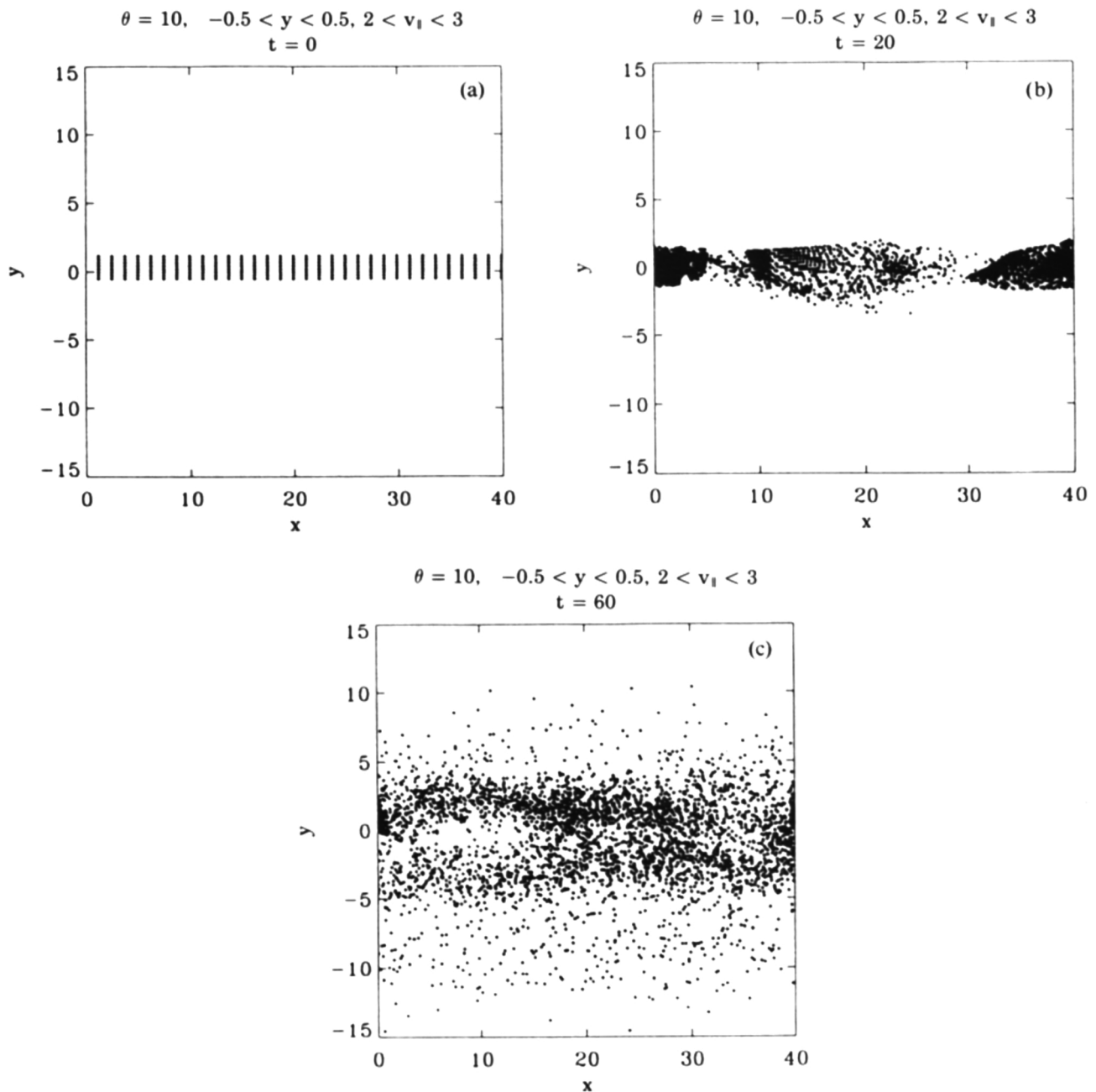


Fig. 12. Evolution of the y - x phase space for the 4096 test particles initially located at $-0.5 < y < 0.5$ at (a) $t = 0$, (b) $t = 20$, and (c) $t = 60$.

diffusion toward the bulk of the distribution function. Even though the beam is injected around $y_b = -6$, particles located around the center $y \approx 0$ experience a strong acceleration simultaneously: By $t = 20$, high negative velocities have been reached. The conservation law in Eq. (11) has the effect of constraining the phase-space excursion of particles in the v_{\parallel} - y space, and this constraint is valid even during chaotic motion.¹³ The rapid formation of a vortex structure diffusing through-

out the v_{\parallel} - x phase space is shown in Fig. 11. Again, at $t = 20$, particles initially located around the center $y \approx 0$ in Fig. 11a show the formation of a strong vortex structure, even though the beam is injected around $y_b = -6$. Other particles at different locations show a similar behavior. The evolution of the test particles in the y - x space is given in Figs. 12 and 13. In Fig. 12c at $t = 60$, the particles, initially located around the center, have diffused throughout the y - x space, while in Fig. 13c,

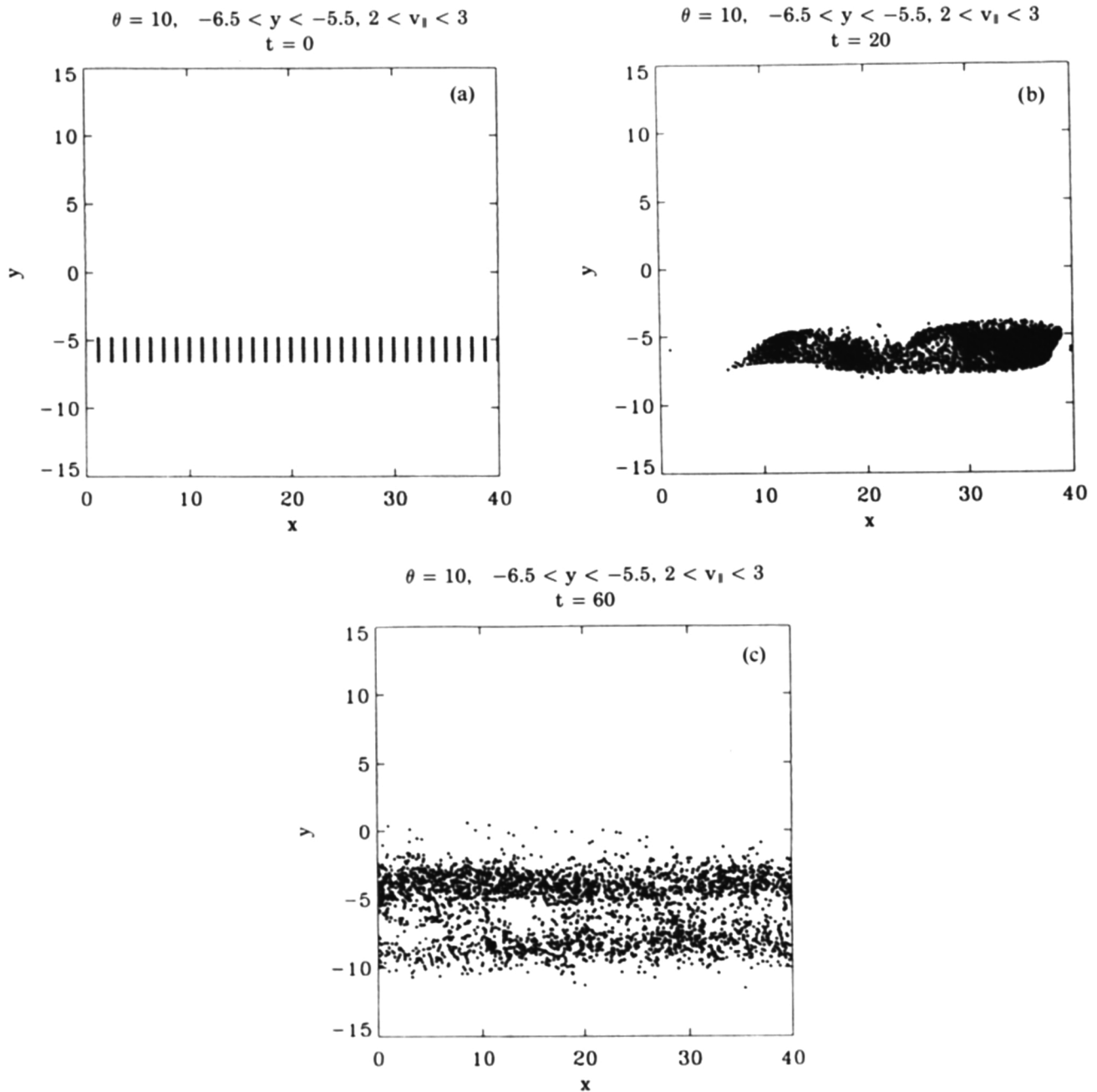


Fig. 13. Evolution of the y - x phase space for the 4096 test particles initially located at $-6.5 < y < -5.5$ at (a) $t = 0$, (b) $t = 20$, and (c) $t = 60$.

the particles initially located in the beam region (where the instability is stronger) are maintaining more cohesion at $t = 60$, diffusing mostly up the density gradient. Similar diffusion toward the center has also been

observed for the more rapid particles located around $v_b = +6$ (in the beam region) in Fig. 4.

We present in Figs. 14 and 15 the time evolution of the distribution functions around positions where the

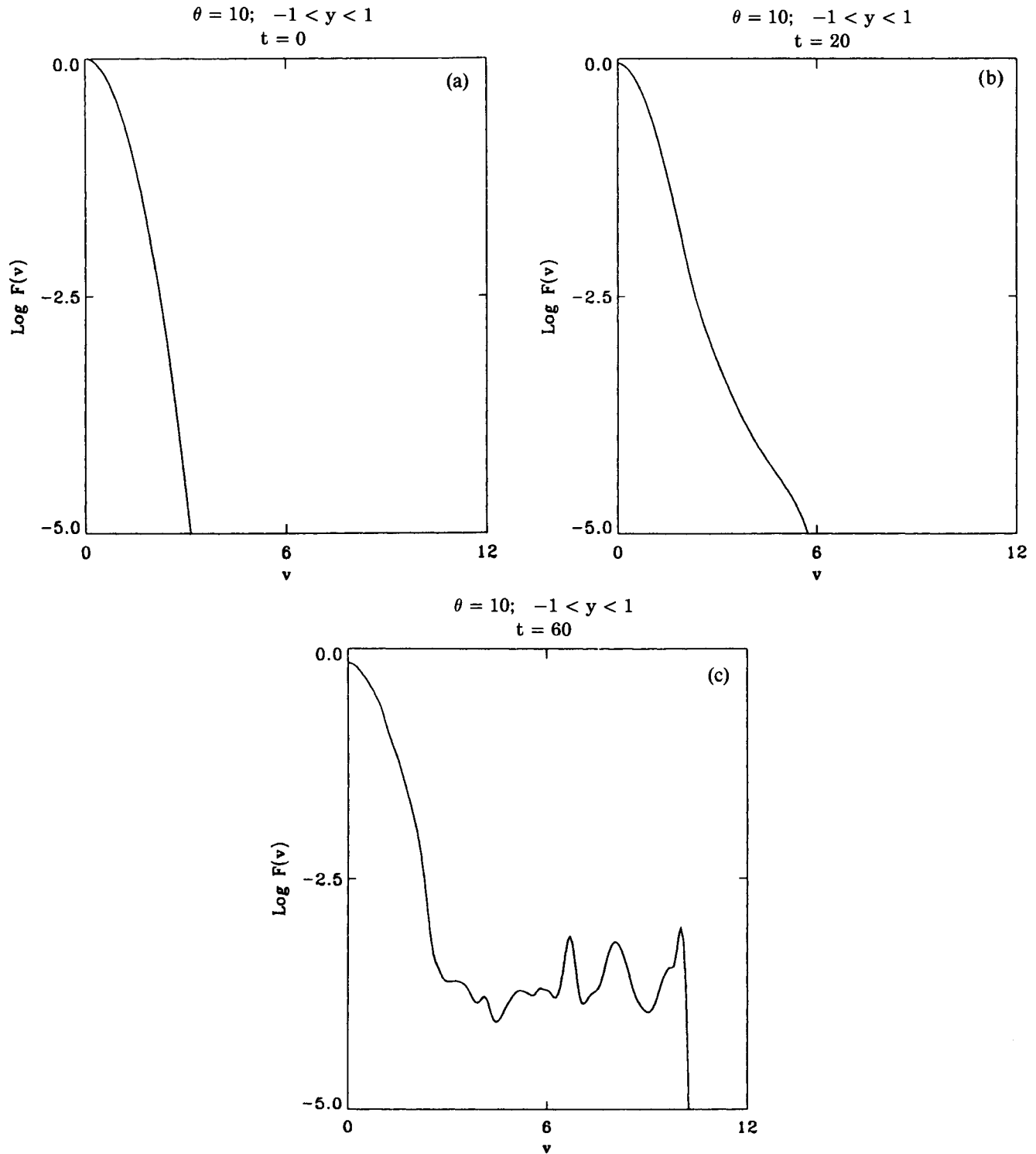


Fig. 14. Time evolution of the spatially averaged distribution function in the slab $-1 < y < 1$ at (a) $t = 0$, (b) $t = 20$, and (c) $t = 60$.

test particles have been followed. These distribution functions are spatially averaged over x , and spatially averaged over a slab in the y direction centered around the position where the test particles were initially po-

sitioned, as indicated in the figures, in a way similar to what has been presented in Eq. (21). Even though the beam contribution in the center is negligible, the distribution function in Fig. 14 shows a strong heating and

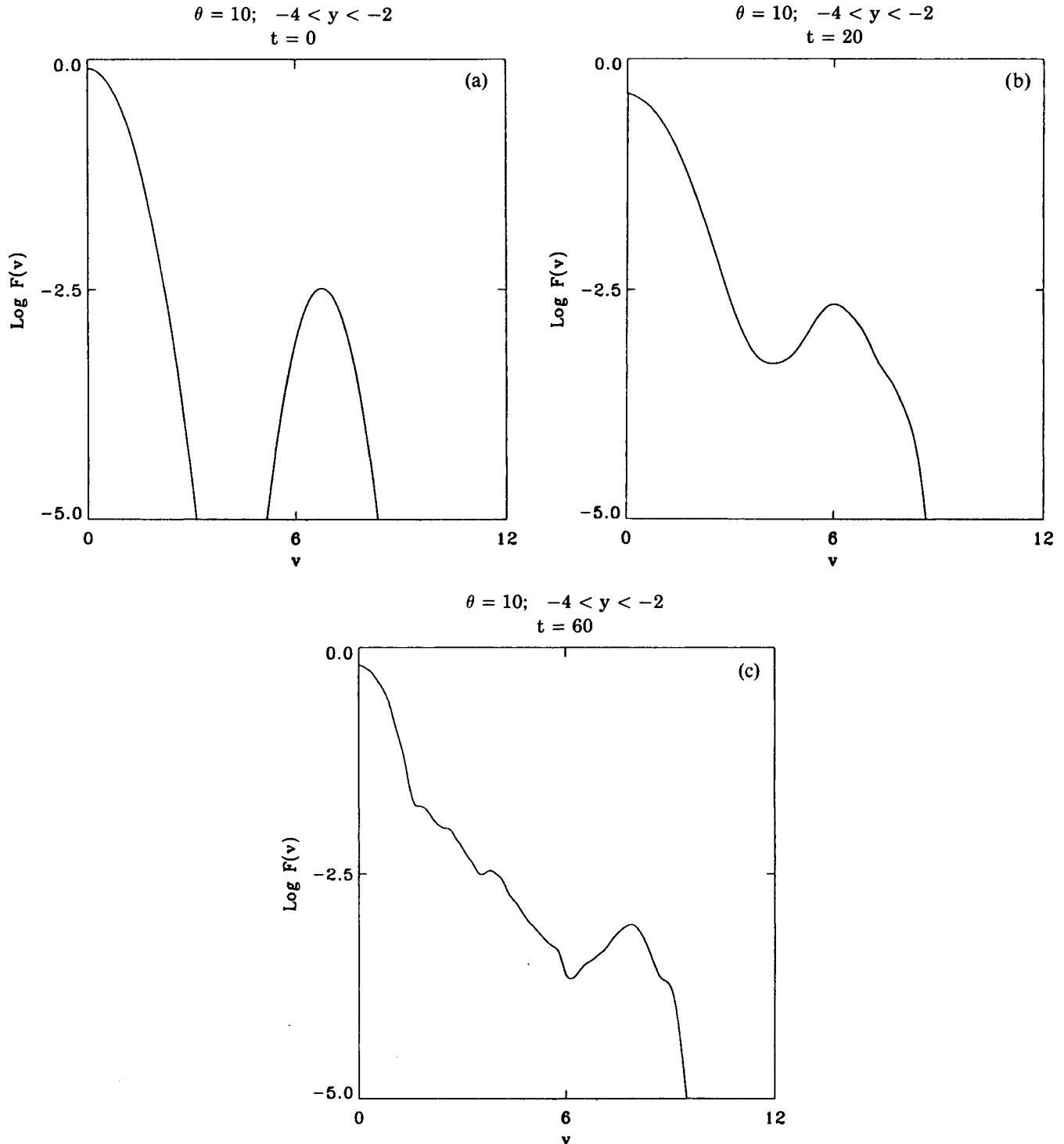


Fig. 15. Time evolution of the spatially averaged distribution function in the slab $-4 < y < -2$ at (a) $t = 0$, (b) $t = 20$, and (c) $t = 60$. (Note the density of the bulk distribution function is decaying the more we move toward the edge of the slab.)

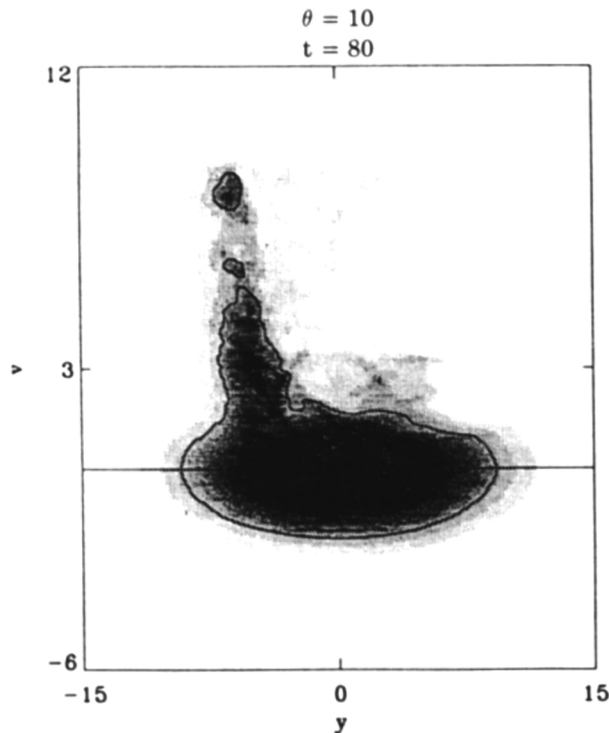


Fig. 16. Shadow plot of the $v_{||}$ - y phase space for the distribution function at $t = 80$.

acceleration of the particles at $t = 20$. The acceleration of the particles toward higher velocities, with the formation of an elongated tail of the distribution function, is apparent in all of Figs. 14 and 15.

Finally, Fig. 16 shows a shadow plot of the distribution function in the phase space $v_{||}$ - y , which clearly shows the heating of the distribution function and the diffusion of the particles in the $v_{||}$ - y phase space (the beam is initially located around $v_b \approx 6$ and $y_b \approx -6$). Figure 17 shows the $v_{||}$ - x phase space, with a huge vortex dominating the region of the tail of the distribution function centered around $v_{||} \sim 5$ as previously discussed.

V. CONCLUSIONS

Collisionless diffusion of particles and current has been studied using a drift-kinetic Vlasov code for the electrons, coupled to a fluid code for the ions. The problem considered was that of an electron beam injected near the edge of a plasma, often referred to as dc helicity injection. The Vlasov approach proves to be effective in eliminating numerical noise, an important requirement to study diffusion processes, while the selective use of test particles provides a graphic description of the evolution of coupled and competing Kelvin-Helmholtz and beam-plasma instabilities. Diffusion in velocity space necessarily causes diffusion in particle trajectory in space. A simple relation connecting the

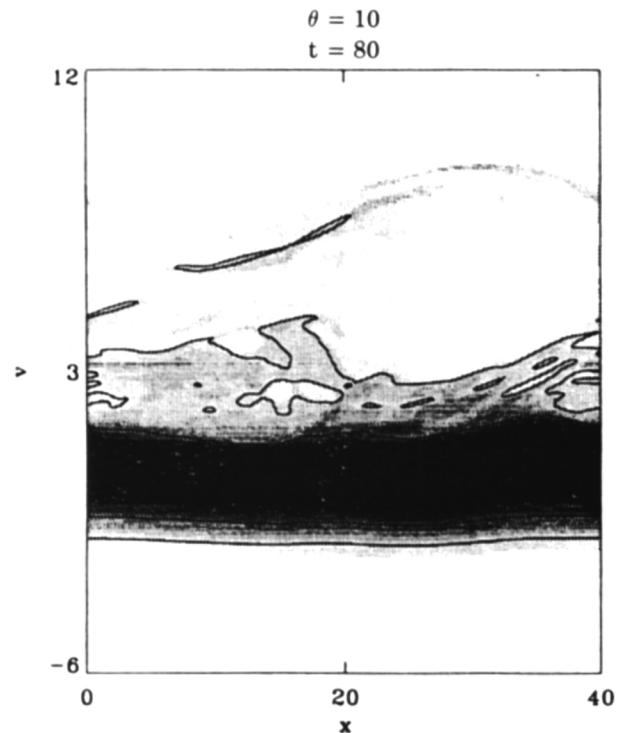


Fig. 17. Shadow plot of the $v_{||}$ - x phase space for the distribution function at $t = 80$.

diffusion in velocity space to the diffusion in space across the magnetic field has been derived for the collisionless plasma considered and verified by numerical simulation. These results are also of relevance to other situations of current drive, in which the beam/plasma interaction is not the driving mechanism. The picture of rapid heating of the plasma bulk coupled with a rapid formation of a tail in the distribution function and diffusion of the current across the magnetic field toward the plasma center is a picture very common in problems when an ohmic electric field is penetrating the plasma and when driving a lower hybrid current in tokamaks. Not only do the present results offer possible explanation to these observations, but also the rapid formation of a plateau shown in Fig. 5 and in Figs. 14, 15, and 16 can add new mechanisms that can help explain the filling of the spectral gap in lower hybrid current drive. A rapidly diffusing hot population is very likely to play a role in this problem. The present simulation offers a qualitative explanation to some of these observations. The very rapid evolution of bump-in-tail instability, coupled with the $\mathbf{E} \times \mathbf{B}$ drift provides a rapid mechanism for the heating and the formation of an elongated tail to the distribution function, coupled to the rapid diffusion of the plateau current toward the plasma center. This coupled effect of beam-plasma and Kelvin-Helmholtz instabilities manifests itself in the plasma center at a time as early as $t = 20$, well before diffusing particles from the edge can reach the plasma

center (see the rapid acceleration and heating of the distribution function in the center in Fig. 14c). Figure 5c at $t = 20$ shows an important heating and acceleration of the particles in the bulk of the distribution function around the center of the slab. Figures 6 and 7 do confirm the formation of an important vortex at $t = 20$ in the x - v_{\parallel} phase space, trapping and accelerating particles.

Collisionless electron heating in a warm plasma in the presence of a fluctuating field has been recently discussed in Ref. 14. In a cold collisionless plasma, each electron samples the electric field at a single location in space, and since the field has a harmonic time variation, it averages to zero everywhere, so no energy can be gained. However, if the electrons are in thermal motion in a warm plasma, or drifting or diffusing by some mechanism, they interact with the field along some trajectory and in general the field does not average to zero along a trajectory. These effects are properly included only in a Vlasov description of the plasma, where the electron trajectory is closely coupled to the field solution, as in the present simulation. Moreover, the problems of fluctuation-driven dissipation mechanism (i.e., turbulent electron viscosity or hyper-resistivity) have been recently discussed using the drift-kinetic Vlasov equation in Ref. 15, which questioned the utility and validity of resistive fluid models for describing present-generation tokamak experiments that operate at very low electron collisionalities. Anomalous electron diffusion is essentially a kinetic effect and is important in understanding the mechanism of electron momentum transport and its impact on current evolution. It plays an important role in the problems of collisionless reconnection and sawtooth crash, and also in anomalous tearing mode growth, reversed-field-pinch relaxation, L-mode anomalous transport in tokamaks, and magnetic reconnection (see Ref. 15).

ACKNOWLEDGMENTS

M. Shoucri is grateful to G. Knorr for many fruitful discussions and to F. Skiff for bringing Ref. 13 to his attention.

The Centre canadien de fusion magnétique is a joint venture of Hydro-Québec, Atomic Energy of Canada Limited (AECL), and the Institut National de la Recherche Scientifique (INRS), in which MPB Technologies and Canatom Inc. also participate. It is principally funded by AECL, Hydro-Québec, and INRS.

REFERENCES

1. M. ONO, G. J. GREENE, D. DARROW, C. FOREST, H. PARK, and T. STIX, "Steady Tokamak Discharge via dc Helicity Injection," *Phys. Rev. Lett.*, **59**, 2165 (1987).
2. A. GHIZZO, B. IZRAR, P. BERTRAND, E. FIJALKOW, M. R. FEIX, and M. SHOUCRI, "Stability of Bernstein-Green-Kruskal Plasma Equilibria. Numerical Experiments Over a Long Time," *Phys. Fluids*, **31**, 1 (1988).
3. A. GHIZZO, M. SHOUCRI, P. BERTRAND, M. FEIX, and E. FIJALKOW, "BGK Structures as Quasi-Particles," *Phys. Fluids*, **129**, 453 (1988).
4. P. BERTRAND, M. FEIX, E. FIJALKOW, P. MINEAU, N. SUH, and M. SHOUCRI, "Nonlinear Evolution of the Beam-Plasma Instability," *Nonlinear Vlasov Plasmas*, F. DOVEIL, Ed., Les Editions de Physique, France (1988).
5. L. Y. CHAN and R. L. STENZEL, "Beam Scattering and Heating at the Front of an Electron Beam Injected into a Plasma," *Phys. Plasma*, **1**, 2063 (1994).
6. H. OKUDA and J. M. DAWSON, "Theory and Numerical Simulation of Plasma Diffusion Across a Magnetic Field," *Phys. Fluids*, **16**, 408 (1973).
7. H. OKUDA, M. ONO, and R. J. ARMSTRONG, "Anomalous Electron Diffusion Across a Magnetic Field in a Beam-Plasma System," *Phys. Fluids*, **31**, 1818 (1988).
8. H. OKUDA and S. HIROE, "Neutral Beam Injection and Plasma Convection in a Magnetic Field," *Phys. Fluids*, **31**, 3312 (1988).
9. A. GHIZZO, P. BERTRAND, M. SHOUCRI, E. FIJALKOW, and M. R. FEIX, "An Eulerian Code for the Study of the Drift-Kinetic Vlasov Equation," *J. Comp. Phys.*, **108**, 105 (1993).
10. A. GHIZZO, P. BERTRAND, M. SHOUCRI, E. FIJALKOW, and M. R. FEIX, "Study of the Diffusion Across a Magnetic Field in a Beam-Plasma Interaction Using a Drift-Kinetic Vlasov Code," *Phys. Fluids*, **B5**, 4312 (1993).
11. P. BERTRAND, A. GHIZZO, S. J. KARTTUNEN, T. PÄTTIKANGAS, R. SALOMAA, M. SHOUCRI, and I. SHKAROFSKY, "Drift-Kinetic Simulations of Wave-Particle Interactions in Lower-Hybrid Current Drive," *Proc. 21st European Physical Society Conf. Controlled Fusion and Plasma Physics*, Montpellier, Vol. III, p. 1082, E. JOFFRIN, P. PLATZ, and P. STOTT, Ed. (1994).
12. A. GHIZZO, M. SHOUCRI, P. BERTRAND, T. W. JOHNSTON, and J. LEBAS "Trajectories of Trapped Particles in the Field of a Plasma Wave Exited by a Stimulated Roman Scattering," *J. Comp. Phys.*, **108**, 373 (1993).
13. F. SKIFF, F. ANDEREGG, T. N. GOOD, P. J. PARIS, M. Q. TRAN, N. RYNN, and R. STERN, "Conservation Laws and Transport in Hamiltonian Chaos," *Phys. Rev. Lett.*, **61**, 2034 (1988).
14. M. M. TURNER, "Collisionless Electron Heating in an Inductively Coupled Discharge," *Phys. Rev. Lett.*, **71**, 1844 (1993).
15. H. BIGLARI and P. H. DIAMOND, "A Mean Field Ohm's Law for Collisionless Plasmas," *Phys. Fluids*, **B5**, 3838 (1993).

G. Manfredi (nuclear engineering, Polytechnic of Torino, 1991; PhD, physics, University of Orléans, France, 1994) works for the United Kingdom Atomic Energy Authority, Government Division. His current research interests are in drift waves, gyrokinetic theory, and plasma accelerators.

M. Shoucri (BSc, electrophysics, Alexandria University, 1965; MSc, engineering, Stanford University, 1970; MSc, 1972, and PhD, 1974, physics, University of Iowa) since 1977 has been at the Research Institute of Hydro-Québec, Québec, and is currently with the Centre canadien de fusion magnétique (CCMF) where his main activity is on numerical simulation problems.

I. Shkarofsky has been the director of the Fusion Technology Division at MPB Technologies, Inc., Quebec, Canada, since 1988. His present interests are in the fields of plasmas, tokamak and laser fusion, and electromagnetic propagation, in particular in transport, collisional effects, kinetic theory, relativistic effects in plasmas, and current drive subject to lower hybrid and electron-cyclotron waves.

Alain Ghizzo (PhD, numerical simulation in plasma physics, 1987; habilitation diploma, University Henri-Poincaré, France, 1993) since 1989 has been with the University Henri-Poincaré as associate professor in the "Laboratoire de Physique des Milieux Ionisés." His research interests are in laser/plasma interactions, the gyrokinetic model for plasma fusion, and the development of new methods of computer simulation in plasma physics via Eulerian Vlasov codes (much of this in collaboration with CCFM; Institut National de la Recherche Scientifique-Energie et Matériaux, Varennes; PPMS-Centre National de la Recherche Scientifique (CNRS) of Orléans, France; and recently the University of Technology of Helsinki).

Pierre Bertrand (PhD, University of Nancy, France, 1972) is currently a full professor at the University Henri-Poincaré, Nancy. He has been performing research in the field of computer experiments in plasma physics. His recent research includes laser/plasma interaction and gyrokinetic models for plasma edge physics in tokamaks.

Eric Fijalkow (MSc, physics on ULF wave propagation in plasma, Technion, Israel, 1968; PhD, ULF and VLF wave propagation, Technion, Israel, 1972) since 1974 has been working at CNRS on problems of plasma simulation.

Marc R. Feix (MS, electrical engineering, Paris, France, 1950; PhD, University of Paris, France, 1958) is the director of research at CNRS.

Seppo Karttunen (Dipl. Ing., 1973, and Dr. Tech., 1979, Helsinki University of Technology) is a senior research scientist at the Energy Research Unit of the Technical Research Center of Finland (VTT Energy). His main interests are nonlinear laser/plasma interactions and radio-frequency-heating physics.

Timo Pattikangas (MSc, engineering, Helsinki University of Technology, Finland, 1988) has worked in the area of wave/particle and wave/wave interactions in a plasma. He has investigated parametric instabilities in fusion plasmas and lower hybrid current drive in tokamaks. Since 1991, he has been working as a research scientist at VTT Energy.

Rainer Salomaa (MSc, engineering, technical physics, 1971, and DrTech, technical physics, 1974, Helsinki University of Technology) is a professor in nuclear engineering at Helsinki University of Technology. His current interests are in radiation physics, laser and plasma physics, and fusion reactors.